The FAD Cofactor of RebC Shifts to an IN Conformation upon Flavin Reduction[†,‡]

Katherine S. Ryan,[§] Sumita Chakraborty,[‖] Annaleise R. Howard-Jones,[⊥] Christopher T. Walsh,[⊥]
and Catherine L. Drennan*,[§]

*Departments of Biology and Chemistry, Massachusetts Institute of Technology, Cambridge, Massachusetts 02139, Department of
Biological Chemistry, University of Michigan, Ann Arbor, Michigan 48109, and Department of Biological Chemistry and
Molecular Pharmacology, Harvard Medical School, Boston, Massachusetts 02115*

ABSTRACT: RebC is a putative flavin hydroxylase functioning together with RebP to carry out a key step in the biosynthesis of rebeccamycin. To probe the mechanism of flavin-based chemistry in RebC, we solved the structure of RebC with reduced flavin. Upon flavin reduction, the RebC crystal undergoes a change in its unit cell dimension concurrent with a 5 Å movement of the isoalloxazine ring, positioning the flavin ring adjacent to the substrate-binding pocket. Additionally, a disordered helix becomes ordered upon flavin reduction, closing off one side of the substrate-binding pocket. This structure, along with previously reported structures, increases our understanding of the RebC enzyme mechanism, indicating that either the reduction of the flavin itself or binding of substrate is sufficient to drive major conformational changes in RebC to generate a closed active site. Our finding that flavin reduction seals the active site such that substrate cannot enter suggests that our reduced flavin RebC structure is off-pathway and that substrate binding is likely to precede flavin reduction during catalysis. Along with kinetic data presented here, these structures suggest that the first cycle of catalysis in RebC may resemble that of *p*-hydroxybenzoate hydroxylase, with substrate binding promoting flavin reduction.

Rebeccamycin, a human DNA-topoisomerase I inhibitor, is a natural product generated in the bacterium *Lechevalieria aerocolonigenes* by the action of eight enzymes: RebF, RebH, RebO, RebD, RebP, RebC, RebG, and RebM (*1−3*). While some Reb enzymes function alone to catalyze discrete steps in the biosynthetic pathway, others function in pairs. Although a complex has not yet been detected experimentally between the two proteins, RebC is required together with RebP, a cytochrome P450 enzyme, to generate the rebecca-mycin aglycon from chlorinated chromopyrrolic acid (*3*) (a net 8-electron oxidation). Because two proteins are required for this conversion, it was unclear from initial studies if RebC played a catalytic role in this process or simply served to modify the activity of RebP. The puzzle arose from the observation that small amounts of product are produced in the absence of RebC when StaP, a close RebP homologue, is used in place of RebP (*4*). This finding suggests that StaP and its homologues are capable of performing all of the necessary chemistry for aglycon formation. In contrast, the addition of RebC to a reaction mixture eliminates the production of side products and promotes the production of the desired product (Figure 1) (*4*), indicating a role for RebC
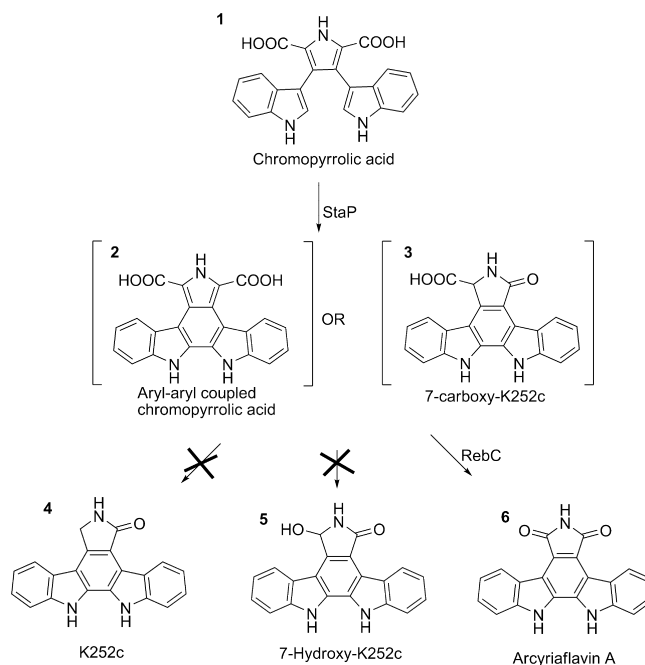

FIGURE 1: Reaction scheme for StaP- (a close homologue of RebP) and RebC-mediated production of the dechloro rebeccamycin aglycon, arcyriaflavin A **6**, from chromopyrrolic acid **1**. StaP alone generates a mixture of products (K252c **4**, 7-OH-K252c **5**, and arcyriaflavin A **6**). By contrast, a single product, arcyriaflavin A **6**, is produced from chromopyrrolic acid **1** by the action of StaP and RebC together. Aryl-aryl coupled chromopyrrolic acid **2** or 7-car-boxy-K252c **3** are proposed products of StaP (*5, 6*).

as an modifying factor. However, recent work suggests that StaP does not produce product directly but rather produces a reactive intermediate that spontaneously forms some
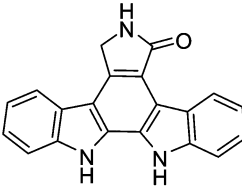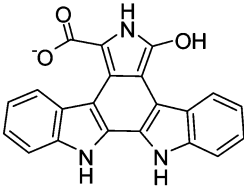
Table 1: Available Structures of RebC

Structure name	Substrate-free	Bound K252c	Bound tautomer of 7-carboxy-K252c	Reduced flavin
PDB ID	2R0C	2R0P	2R0G	3EPT
Resolution	1.8 Å	2.1 Å	2.4 Å	3.0 Å
Bound cofactor	FAD	FAD	FAD	FADH⁻
Unit cell volume (Å³)	302,000	299,000	620,000	602,000
Unit cell dimensions				
a (Å)	63.2	63.1	64.9	63.3
b (Å)	77.6	77.5	78.4	78.2
c (Å)	64.7	64.7	123.6	123.1
β (°)	108.0	108.9	99.6	98.7
Bound indolocarbazole	-	K252c	tautomer of 7-carboxy-K252c	-
Flavin position	OUT	OUT	IN	IN
Helix ordering	disordered	ordered	ordered	ordered

product over time (*5*). When RebC is present, this reactive intermediate is sequestered in the RebC active site, preventing its decomposition, and is then converted enzymatically to the rebeccamycin aglycon (*5, 6*). Specifically, RebC is thought to be a flavin-dependent hydroxylase that reacts with putative substrates, aryl-aryl coupled chromopyrrolic acid **2** and/or 7-carboxy-K252c **3**, produced by the RebP homologue StaP (*5−7*). Given the reactivity of both molecules, however, the ability of either to act as a RebC substrate is difficult to test directly (*5*).[1]

Due to the instability of the putative substrate molecule(s), we have chosen a largely crystallographic approach to study RebC, publishing three crystal structures prior to this work (*6*). These RebC structures include a substrate-free form, a structure with a tautomer of 7-carboxy-K252c **3** bound in the active site, and a structure with K252c **4** bound in the active site (Table 1). These structures show that RebC is structurally homologous to members of the flavin-dependent hydroxylase family (*8−11*) such as the well-studied *p*-hydroxybenzoate hydroxylase (*p*HBH) (*12*). A comparison of substrate-free and bound structures of RebC shows that the binding of molecules into the active site elicits a change in residues 354−363. These residues, which are adjacent to the substrate-binding pocket, are disordered in the substrate-free structure and become ordered as part of a helix in the two structures with bound indolocarbazoles (Table 1). This

helix, including residues 354−363, is termed the "melting helix", reflecting its ability to change states (ordered or disordered) depending on the conditions. The melting of this helix is thought provide the route by which substrates enter and products depart the active site (*6*). The presence of a "melting helix" contrasts with its structural homologue, *p*-hydroxybenzoate hydroxylase, which uses a third conformation of the flavin, an OPEN conformation, to enable entry to the active site (*13*).

Structural comparisons also show that the FAD can adopt two conformations in RebC: an OUT conformation in which the isoalloxazine of FAD is more solvent accessible and an IN conformation where the isoalloxazine is more secluded from solvent and positioned to interact with bound substrate-like molecules. *p*HBH also utilizes a "mobile flavin" in its reaction mechanism (*8*). Interestingly, not all substrate-like molecules elicit a change in FAD conformation from OUT to IN in RebC. The isoalloxazine of FAD is IN in the structure with 7-carboxy-K252c **3** bound but is OUT when K252c **4** is bound. This difference in observed FAD conformation may reflect the fact that 7-carboxy-K252c **3** is, or more closely resembles, the true substrate of RebC. While K252c **4** is known not to be a substrate (*4*), 7-carboxy-K252c **3** is too reactive to be tested conveniently as a possible substrate (*5*). We were only able to obtain the structure of 7-carboxy-K252c **3** bound RebC by soaking crystals in a mixture of chromopyrrolic acid **1** degradation products for a week. Over this time period, 7-carboxy-K252c **3** selectively accumulates in the active site of crystallized RebC, allowing for its structural characterization. This selectivity of RebC for 7-carboxy-K252c **3** over a mixture of chromopyrrolic acid degradation products is consistent with the idea that 7-carboxy-K252c **3** may closely resemble or be the RebC substrate.

---

[1] Abbreviations: FAD, flavin adenine dinucleotide; FADH⁻, reduced flavin adenine dinucleotide; tautomer of 7-carboxy-K252c **3**, 7-carboxy-5-hydroxy-12,13-dihydro-5*H*-indolo[2,3-*a*]pyrrolo[3,4-*c*]carbazole; aryl-aryl-coupled chromopyrrolic acid **2**, 5,7-dicarboxy-12,13-dihydro-5*H*-indolo[2,3-*a*]pyrrolo[3,4-*c*]carbazole; K252c **4**, 6,7,12,13-tetrahydro-5*H*-indolo[2,3-*a*]pyrrolo[3,4-*c*]carbazol-5-one; 7-hydroxy-K252c **5**, 7-hydroxy-6,12,13-trihydro-5*H*-indolo[2,3-*a*]pyrrolo[3,4-*c*]carbazole; arcyriaflavin A **6**, 12,13-dihydro-5*H*-indolo[2,3-*a*]pyrrolo[3,4-*c*]carbazole-5,7(6*H*)-dione; *p*HBH, *p*-hydroxybenzoate hydroxylase; pOHB, *p*-hydroxybenzoate.

Like the FAD in RebC, the isoalloxazine in *p*HBH shifts to an IN conformation when substrate is bound. Substrate binding to *p*HBH also dramatically affects the rate of reduction of the FAD by NADPH. When NADPH binds to a *p*HBH–*p*OHB complex, spectral shifts indicate that the FAD moves from IN to OUT, positioned for the N5 of the isoalloxazine to accept a hydride from NADPH. Upon FAD reduction, crystallographic data tell us that the FADH⁻ of *p*HBH moves back to an IN conformation where it can react with molecular oxygen and substrate. To examine the structural effect of FAD reduction in RebC, we have determined the structure of RebC with fully reduced flavin. Although we do not know the protonation state of reduced flavin from our structure, we will assume in this report that it is FADH⁻, and not $FADH_2$, consistent with the typical protonation state of FAD in this family of proteins (*14, 15*). Here we find reduced flavin in RebC in an IN conformation, with the "melting helix" ordered. This structure, which we will call the "reduced-RebC" structure, is very similar to the structure of RebC with a bound tautomer of putative substrate 7-carboxy-K252c **3**, suggesting that either reduction of the flavin *or* appropriate positioning of a carboxylate-containing substrate such as the tautomer of 7-carboxy-K252c **3** is sufficient to trigger the movement of the isoalloxazine to the IN position and to cause the "melting helix" to form, sealing off the substrate-binding pocket. We have also examined the rate of reduction of FAD in RebC by NADH in the absence of substrate and find that like *p*HBH the rate is slow. These new findings, along with the previous structural work on RebC, allow for a detailed comparison of putative flavin hydroxylase RebC with *p*HBH, one of the better studied family members.

MATERIALS AND METHODS

Sample Preparation. RebC protein was prepared and crystallized as described earlier (*4, 6*). Reduced RebC was generated by incubating a RebC crystal in a cryogenic solution (19% PEG-8000, 0.1 M HEPES, pH 7.4, 20% glycerol) and adding an amount of solid sodium dithionite that is in slight excess of the point at which the crystal became completely clear, indicating that all FAD was reduced. The crystal was then flash-frozen in liquid nitrogen.

Data Collection and Processing and Structure Determination. Data were collected at beamline 9-2 at the Stanford Synchrotron Radiation Laboratory, integrated in HKL2000, and scaled in Scalepack (*16*) without σ cutoff. The unit cell volume of reduced RebC is 602000 Å³, almost twice the volume of substrate-free RebC, because two monomers previously related by a crystallographic 180° rotation shift to be related by a 160° rotation, with consequent alteration of the *a*, *c*, and *β* values of the unit cell (Table 1). Data collection statistics are shown in Table 2. The structure of reduced RebC was solved in CNS (*17*), using rigid-body refinement and the coordinates from PDB ID 2R0G, with reflections flagged as "free" identically to the structure factor file used in refinement of PDB ID 2R0G. Only coordinates for protein atoms were used in rigid-body refinement, with coordinates for water molecules and flavin molecules added later in refinement. Following rigid-body refinement, multiple rounds of refinement, including simulated annealing, were carried out in CNS with alternate rounds of manual adjust-

Table 2: Data Collection and Refinement Statistics for the Reduced-RebC Structure

Data Collection	
beamline	SSRL, 9-2
wavelength (Å)	0.9797
space group	$P2_1$
unit cell	
a, b, c (Å)	63.3, 78.2, 123.1
β (deg)	98.7
resolution (Å)[a]	40.0–2.97 (3.08–2.97)
completeness (%)[a]	90.4 (50.7)
$I/\sigma I$[a]	9.9 (3.0)
redundancy[a]	4.1 (3.1)
unique reflections	22485 (1255)
R_{sym}[a,b]	0.149 (0.270)

Refinement	
resolution range (Å)	40.0–2.97
R_{cryst} (%)[c]	22.5
R_{free} (%)[c]	27.6
no. of non-hydrogen atoms	
protein	7913
FADH⁻	106
water	65
Na⁺	1
average *B*-factors (Å²)	
protein	46.7
FADH⁻	38.6
water	23.4
Na⁺	23.6
rmsd[d] bond length (Å)	0.008
rmsd[d] bond angle (deg)	1.34
Ramachandran plot (% residues)	
most favored	85.2
additionally allowed	14.1
generously allowed	0.5
disallowed	0.2

[a] Values in parentheses indicate highest resolution bin. [b] $R_{sym} = (\sum_i \sum_{hkl} |I_i(hkl) - \langle I(hkl)\rangle|)/\sum_{hkl}\langle I(hkl)\rangle$, where $I_i(hkl)$ is the intensity of the *i*th measured reflection and $\langle I(hkl)\rangle$ is the mean intensity for the reflection with the Miller index (*hkl*). [c] $R_{cryst} = (\sum_{hkl} ||F_o(hkl)| - |F_c(hkl)||)/\sum_{hkl}|F_o(hkl)|$; R_{free} is calculated identically, using 5% of reflections omitted from refinement. [d] Root mean squared deviation.

ment carried out in COOT (*18*). We found no notable differences between the two molecules of RebC in the asymmetric unit, regardless of whether or not noncrystallographic symmetry (NCS) restraints were used. However, to improve the data to parameter ratio, NCS restraints were used throughout refinement. The topology and parameter files for reduced flavin were generated from the $FADH_2$ molecule in the PrnA structure (PDB ID 2ARD) (*19*) as well as a higher resolution FAD molecule from cholesterol oxidase (PDB ID 1N4V) (*20*), using XPLO2D (*21*). A composite omit map was used to verify the overall structure, with omit maps also generated for the flavin cofactor and the "melting helix". There are two protein chains in the asymmetric unit, each containing 529 residues from RebC with 20 amino acids in an N-terminal tag. RebC residues 3–529 from chain A and 2–529 from chain B are included in the final model, with residues 247–250 and 417–423 disordered in chain A and residues 247–250 and 418–421 disordered in chain B. There is also one molecule of reduced flavin in each active site. One sodium atom, positioned near an aspartate, was included in the model. When instead modeled as water, its *B*-factor was atypically low (5 Å²). More residues are outside of the "most favored" region of a Ramachandran plot than has been observed for other RebC structures (*6*); this is likely a reflection of the lower resolution of these data relative to

other RebC structures (Table 1). Refinement statistics for the reduced-RebC structure are shown in Table 2.

Analysis of Surface Accessibility of the Substrate-Binding Pocket. CAVER (*22*) was used to determine if any pathways connected the substrate-binding pocket of RebC to external solvent, with subsequent examination of results in PYMOL (http://pymol.sourceforge.net). Based on the representation of this pathway as spheres with varying radii, the widest pathway identified that leads to solvent in the reduced-RebC structure is too narrow for a putative RebC substrate to traverse.

Determination of Rate Constant for Reduction of FAD in the Absence of Substrate under Single Turnover Conditions. RebC was diluted in 150 mM NaCl, 10% glycerol, and 25 mM HEPES, pH 7.5, in a glass tonometer and made anaerobic by ~15 alternate cycles of incubation with purified argon gas and purging by vacuum. 3,4-Dihydroxybenzoate and protocatechuate 3,4-dioxygenase were included to scavenge any residual oxygen (*23*). A stock solution of 13 mM NADH was prepared in unneutralized Tris base, and dilutions were made into the RebC buffer (150 mM NaCl, 10% glycerol, 25 mM HEPES, pH 7.5). All NADH solutions were bubbled with argon for >15 min prior to use. A Hi-Tech DX-2 stopped-flow spectrophotometer (Bradford on Avon, U.K.) was incubated with an anaerobic solution of 3,4-dihydroxybenzoate and protocatechuate 3,4-dioxygenase overnight prior to use. The tonometer containing the enzyme was connected to one syringe and the buffer or NADH solution was connected to the second syringe of the stopped-flow spectrophotometer. Detection was with a photomultiplier, and spectra were recorded at approximately 5 min intervals. Data were analyzed using KinetAsyst 3.16.

RESULTS

Unit Cell Dimensions Change. RebC crystals grown from recombinantly expressed and purified protein have unit cell dimensions of $a = 63.2$ Å, $b = 77.6$ Å, $c = 64.7$ Å, and $\beta = 108.0°$ (space group $P2_1$) with one monomer per asymmetric unit (PDB ID 2R0C) and appear yellow throughout data collection (*6*). However, upon incubation of these crystals with dithionite, the crystals lose their yellow color and assume alternate unit cell dimensions of $a = 63.3$ Å, $b = 78.2$ Å, $c = 123.1$ Å, and $\beta = 98.7°$ (space group $P2_1$) with two monomers per asymmetric unit. The cell dimension change occurs when two chains, previously related by a crystallographic 180° rotation, shift relative positions such that they are related by a 160° rotation. The unit cell dimensions of the sodium dithionite-reduced crystals are similar to the unit cell dimensions observed from RebC with a bound tautomer of 7-carboxy-K252c **3** (PDB ID 2R0G), which also changes cell dimensions relative to the substrate-free structure and has unit cell dimensions of $a = 64.9$ Å, $b = 78.4$ Å, $c = 123.6$ Å, and $\beta = 99.6°$ (space group $P2_1$) (*6*). Unlike the RebC crystals with a bound tautomer of 7-carboxy-K252c **3**, however, which diffracted to 2.4 Å resolution (*6*), sodium dithionite-soaked RebC crystals generally gave poorer quality data, with the best data obtained reported here (2.97 Å resolution). The change in unit cell dimensions must occur over a short period of time (less than a few minutes) in the case of sodium dithionite soaking of RebC, whereas the accumulation of the tautomer of 7-car-

boxy-K252c **3** in the active site of RebC takes much longer (an entire week) (*6*). It is possible that the rapid change in unit cell dimensions caused by soaking in the presence of sodium dithionite resulted in the lower quality data achieved for the reduced-RebC structure compared to the structure of RebC with a bound tautomer of 7-carboxy-K252c **3** (Table 1).

The FAD Cofactor Moves IN upon Reduction. The similarities of the reduced-RebC structure to that of FAD-RebC with a bound tautomer of 7-carboxy-K252c **3** extend to the positioning of the isoalloxazine in the active site. In the structure of FAD-RebC with a bound tautomer of 7-carboxy-K252c **3**, the FAD is observed in the IN conformation, adjacent to the bound molecule in the substrate-binding pocket. Likewise, the reduced flavin in the reduced-RebC structure is also observed in the IN conformation (Supporting Information Figure 1). The positioning of the cofactor in the reduced-RebC structure and in the structure of FAD-RebC in complex with a tautomer of 7-carboxy-K252c **3** is different from the substrate-free and K252c **4**-soaked structures, where the FAD is observed in the OUT conformation (Table 1, Figure 2A). Hence, after reduction by dithionite, the reduced isoalloxazine of the flavin cofactor moves approximately 5 Å on the pivot of the pyrophosphate phosphate moiety proximal to the flavin from the OUT to the IN position (Figure 2A, Supporting Information Figure 2).

The Overall Structure Is Highly Similar to the Structure of RebC with a Bound Tautomer of 7-Carboxy-K252c. The root mean squared deviation (rmsd) distance between the reduced-RebC and structure of RebC with a bound tautomer of 7-carboxy-K252c **3** is 0.66 Å for 514 Cα carbon atoms. By comparison, the rmsd variations in distances between the reduced RebC and FAD-RebC with bound K252c **4** structure is 0.82 Å for 504 Cα carbon atoms, and the rmsd between the reduced RebC and the FAD-RebC substrate-free structure is 1.02 Å for 494 Cα carbon atoms. The active sites themselves of the reduced-RebC structure and structure of FAD-RebC with a bound tautomer of 7-carboxy-K252c **3** also are nearly superimposable, with one key exception: no substrate molecule is bound in the reduced-RebC structure (Figure 2C,D). Interestingly, even the "melting helix", a helix that is disordered in the substrate-free structure, which becomes ordered in the structures of RebC with bound K252c **4** and with the bound tautomer of 7-carboxy-K252c **3** (Figure 2F), also becomes ordered in reduced RebC, despite the lack of a substrate-like molecule in the substrate-binding pocket (Figure 2B,E, Supporting Information Figure 3).

The Substrate-Binding Pocket Is Inaccessible to Substrate upon Flavin Reduction. To determine if an indolocarbazole-like substrate could enter the binding pocket in a reduced-RebC state, the program CAVER was used (*22*) to identify the favored path by which a probe placed in the active site would escape to the solvent. The four available structures of RebC (2R0C, 2R0G, 2R0P, and 3EPT, the reduced-RebC structure presented here) were analyzed, with bound molecules in the active site removed for 2R0G and 2R0P. The substrate-free RebC structure (2R0C) showed the most solvent accessible pathway, with a probe placed in the active site moving immediately to the solvent, via the disordered, "melted helix", between residues 354−363 (Figure 3A,B). By contrast, for the other three structures, each of which
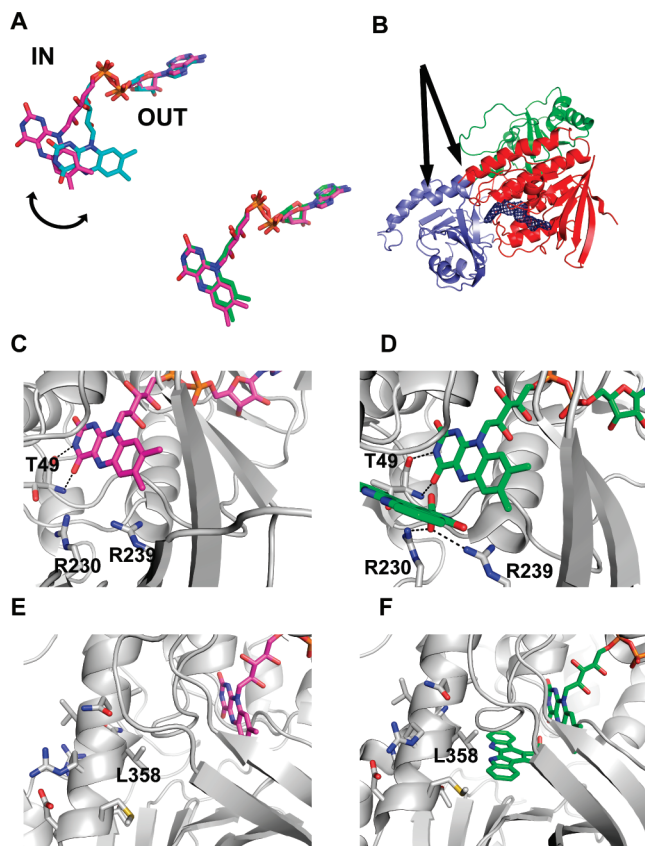
FIGURE 2: Structural comparisons between reduced-RebC and other RebC structures. (A) Reduced flavin from the reduced-RebC structure (this work) is shown with magenta carbons, FAD from the substrate-free structure (PDB ID 2R0C) is shown with blue carbons, and FAD from the structure of RebC with a bound tautomer of 7-carboxy-K252c **3** (PDB ID 2R0G) is shown with green carbons. Top: Reduced flavin from the reduced-RebC structure superimposed with FAD from the substrate-free structure. Bottom: Reduced flavin from the reduced-RebC structure superimposed with FAD from the RebC structure with a bound tautomer of 7-carboxy-K252c **3**. (B) Structure of reduced-RebC colored red (domain I, cofactor-binding domain), blue (domain II, base of substrate-binding pocket), and green (domain III, thioredoxin-like domain). Blue composite omit density is contoured at 1.4σ around the reduced flavin molecule (see Supporting Information Figure 1 for stereoviews). Arrows indicate the boundaries of the "melting helix", which is ordered in this structure (see Supporting Information Figure 3 for omit density of melting helix). (C) Active site of the reduced-RebC structure, with dashes indicating hydrogen-bonding interactions. (D) Active site of RebC with a bound tautomer of 7-carboxy-K252c **3** (PDB ID 2R0G) with dashes indicating hydrogen-bonding interactions. (E) The "melting helix" from the reduced-RebC structure is shown with side-chain atoms as sticks, with leucine-358 labeled. (F) The "melting helix" from the RebC structure with a bound tautomer of 7-carboxy-K252c **3** (PDB ID 2R0G) is shown with side-chain atoms as sticks. Leucine-358 is less than 4 Å from the bound tautomer of 7-carboxy-K252c **3**.

contains a formed helix between residues 354−363 (Figure 3C,D), the pathway from the substrate-binding site to external solvent is via another side of the active site (Figure 3E). However, based on examination of the results in PYMOL, this pathway is unlikely to be wide enough near the active site for an indolocarbazole-like molecule to traverse to the surface of the enzyme (Figure 3E,F). This pathway is also the widest route to the substrate-binding site from the surface of the protein in the reduced-RebC structure. We suggest that an indolocarbazole-sized molecule would require an opening with a radius of at least 4.5 Å; however, the pathway
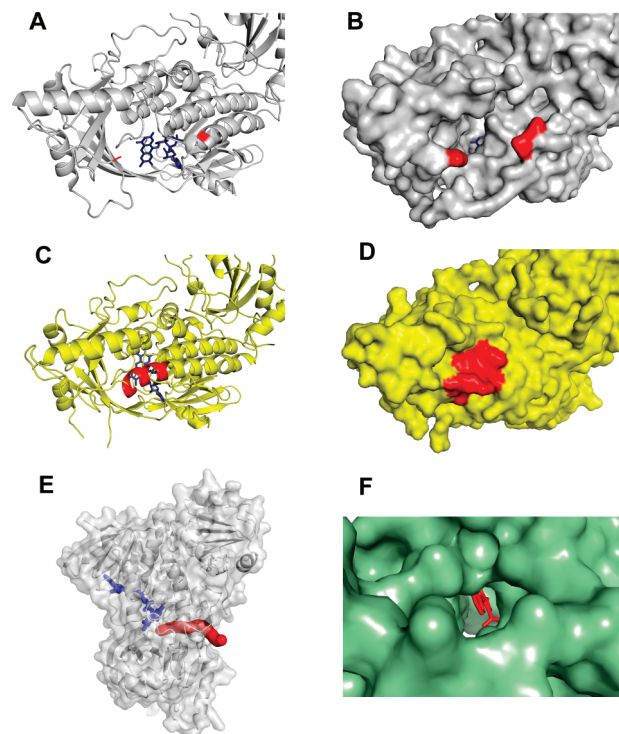

FIGURE 3: Access to the substrate-binding pocket. (A) In the substrate-free structure of RebC, residues 354−363 of the "melting helix" are disordered. The boundaries of this region are shown in red. FAD is shown with blue sticks. (B) Surface representation of the structure in (A). Part of the FAD molecule (blue sticks) can be seen inside the structure. (C) An identical view of the reduced-RebC structure with the "melting helix" in red. (D) Surface representation of the reduced-RebC structure shown in (B). (E) With the "melting helix" ordered a pathway traced to external solvent from the active site of reduced RebC. Protein is in gray with the surface traced. Flavin is depicted in thick blue sticks, and the pathway is shown with red spheres. (F) The same pathway can be traced from the active site of the structure of RebC with a bound tautomer of 7-carboxy-K252c **3** and the "melting helix" ordered. The protein surface is shown in pale green, with the tautomer of 7-carboxy-K252c **3** shown in red. This entryway to the substrate-binding site is likely too narrow for a substrate-like molecule to traverse.

out of the reduced-RebC structure from where a substrate would be positioned does not become 4.5 Å wide until just before the surface of the enzyme.

Reduction of RebC Is Slow in the Absence of Substrate. Previous studies have shown that NADH is the preferred reductant for RebC in the two-enzyme conversion of chromopyrrolic acid **1** to arcyriaflavin A **6** (*4*). To investigate the rate constant of reduction of the FAD in RebC by NADH, we used a stopped-flow spectrophotometer and analyzed the reduction of FAD (by monitoring A_{450}). Reduction was extremely slow, and in retrospect, the use of a stopped-flow spectrophotometer to determine the rate constant was unnecessary. However, using an extremely high concentration of NADH (1 mM), the rate constant for reduction was determined as 0.0023 s^{-1} (Supporting Information Table 1), an extremely slow rate.

DISCUSSION

Our structure of reduced-RebC provides insight into the catalytic cycle of RebC. The structure of reduced RebC contains flavin in an IN conformation and contains an ordered

Table 3: Experimental Evidence for States of *p*-Hydroxybenzoate Hydroxylase Catalytic Cycle

state	description of state	position of flavin	crystallographically observed	PDB ID	biochemical evidence
1	substrate-free	OPEN−IN equilibrium	yes, but as R220Q mutant	1K0L (13)	slow substrate binding but otherwise unchanged catalysis of E49N mutant suggests two interconverting states (29); R220Q mutant more stable in OPEN than IN state (25); single molecule studies on substrate-free *p*HBH (30)
2	substrate-bound	IN	yes	1PBE (26)	
3	substrate-bound, NADPH-bound	transition to OUT	no, but R220Q mutant observed with NADPH (no substrate) and wild type with alternate substrate observed in OUT conformation	1K0J (13), 1DOD (8, 28)	spectral shifts on flavin movement to the OUT position; R220K mutant stabilized in OUT conformation (31)
4	substrate-bound, FADH⁻, NADP⁺-bound	OUT	no, but R220Q mutant observed with NADPH (no substrate)	1K0J (13)	
5	substrate-bound, FADH⁻	IN	yes	not deposited (27)	movement of reduced flavin to IN conformation driven by positive electrostatic field as shown by K297M mutant (15)
6	substrate-bound, flavin-C4a-O-OH	IN	no		observed spectroscopically (32)
7	product bound, flavin-C4a-OH	transition to OPEN	yes, but with product bound, FAD complex	1PHH (33)	observed spectroscopically (32)

helix adjacent to the substrate-binding pocket. Substrate-free RebC, by contrast, which was used to generate the reduced RebC by soaking with a dithionite solution, has flavin in an OUT conformation and a disordered, "melting helix". Thus, reduction of the cofactor causes the isoalloxazine to move IN and the "melting helix" to become ordered. Together with another structure of RebC, that of RebC with a bound tautomer of 7-carboxy-K252c **3**, where flavin is IN and the "melting helix" is ordered, we now have several crystallographic "snapshots" of this interesting enzyme (Tables 1 and 4). One structure we do not yet have is that of reduced RebC with a bound tautomer of 7-carboxy-K252c **3**. Obtaining such a structure may be difficult given that both steps involved, the week-long soak with chromopyrrolic acid **1** and reduction with dithionite, lead to significant losses in resolution. Although we do not have a structure of reduced-RebC with a bound tautomer of 7-carboxy-K252c **3**, we expect that such a structure would be nearly identical to the structure of FAD-RebC with a bound tautomer of 7-carboxy-K252c **3**, given that flavin reduction and substrate binding each bring about similar conformational changes in RebC.

Despite these various crystallographic "snapshots" of RebC, questions remain about the mechanism of RebC, largely because its putative substrates are too reactive for convenient enzymatic study. Hypothetical reaction schemes of RebC with putative substrates 7-carboxy-K252c **3** or aryl-aryl coupled chromopyrrolic acid **2** suggest that RebC may have to carry out multiple rounds of oxidative chemistry to generate the rebeccamycin aglycon, but few wild-type flavin hydroxylases are capable of doing multiple rounds of flavin-based catalytic chemistry on a single substrate molecule. One interesting enzyme to compare with RebC might be salicylate hydroxylase, which catalyzes both hydroxylation and decarboxylation reactions of its substrate (7, 24); however, many mechanistic details are lacking for this enzyme. In any case, the possibility that RebC, like other flavin hydroxylases, carries out only one round of catalysis on its substrate is still a reasonable hypothesis if the remainder of the chemistry is spontaneous in aerobic conditions and results in only the desired final product. Because of the many unknowns in the catalytic cycle of RebC, it makes sense to think about a single round of catalysis in comparison to the best studied flavin hydroxylase enzyme, *p*-hydroxybenzoate hydroxylase.

p-Hydroxybenzoate hydroxylase, the canonical flavin-dependent hydroxylase, is thought to carry out a flavin-based hydroxylation of its substrate through at least seven states (Supporting Information Figure 4). The details of these states have been elucidated using a combination of stopped-flow spectroscopy and X-ray crystallography (Table 3). In brief, *p*HBH, initially existing with oxidized flavin in a dynamic equilibrium between the OPEN and IN positions (state 1), captures a molecule of *p*-hydroxybenzoate (*p*OHB) while in the OPEN conformation, an additional conformation of the flavin that enables entry of substrate and departure of product in *p*HBH (25). Substrate binding then shifts the equilibrium of the isoalloxazine toward the IN conformation (state 2), a state that is represented by one of the original structures of *p*HBH, where *p*OHB was bound to *p*HBH (26). When NADPH binds the enzyme containing bound *p*OHB, the flavin is triggered to move to the OUT conformation (state 3) where the N5 of the isoalloxazine is positioned optimally to receive a hydride from NADPH; this transition only occurs when substrate is bound. Upon reduction of the FAD by NADPH (state 4), NADP⁺ is released. The resultant FADH⁻ anion shifts to the IN position due to the positive electrostatic field near the IN position (state 5); the structure of *p*HBH with reduced flavin and bound substrate (obtained using anoxygenic solutions) represents this state (27). Next, flavin reacts with oxygen and hydroxylates the bound *p*OHB, while in the IN conformation (states 6 and 7). Finally, the resulting product, 2,3-dihydroxybenzoate, is released via the OPEN conformation, and loss of H_2O returns the FAD cofactor to its oxidized form and *p*HBH to the initial state (state 1), which is a dynamic equilibrium between the OPEN and IN positions (12). Table 3 describes the experimental support for each step of this scheme, including those states which have been observed crystallographically.

Table 4: Proposed States of the RebC Catalytic Cycle

state in RebC catalytic cycle	description of state	position of flavin	state of the "melting" helix	crystallographically observed	PDB ID
1	substrate-free	OUT	disordered	yes	2R0C
2	substrate-bound	IN	ordered	yes	2R0G
3	substrate-bound, NADH-bound	unknown	unknown	no	
4	substrate-bound, FADH$^-$, NAD$^+$-bound	unknown	unknown	no	
5	substrate-bound, FADH$^-$	IN	ordered	no, but substrate-free reduced-RebC structure is suggestive of IN conformation	3EPT
6	substrate-bound, flavin-C4a-O-OH	unknown	unknown	no	
7	product-bound, flavin-C4a-OH	unknown	unknown	no	

Our crystallographic observations have collectively captured three states of RebC. Using the known reaction mechanism for *p*HBH, we can begin to piece together a likely reaction cycle for one round of flavin-based hydroxylation in RebC (Table 4). The first state we have captured is state 1, prior to substrate binding. In this stage, the flavin is OUT and the "melting helix" is disordered. In contrast to *p*HBH, where a third conformation of the flavin, the OPEN conformation, is thought to enable entry of substrate and departure of product, in RebC, we believe the "melting helix" is instead the route for substrate entry and product departure. Unlike *p*-hydroxybenzoate, the putative RebC substrate is too large to enter the active site through a flavin OPEN conformation. Additionally, in contrast to the flavin in *p*HBH, the RebC flavin is OUT prior to substrate binding. The second state we have captured is a state 2 conformation, where substrate is bound. In this state, the flavin is IN (as is true in *p*HBH) and the "melting helix" is ordered. The third state we have captured is likely off-pathway, having bound reduced flavin but no bound substrate. This structure is suggestive of a state 5-like conformation, where flavin is reduced and substrate is bound. Although there is no substrate bound in this structure, the "melting helix" is ordered, and substrate would be unable to enter. Therefore, although no actual substrate molecule is present in this structure, RebC appears to assume a conformation as though a substrate molecule were bound; i.e., this reduced-RebC structure seems to represent a stage in the catalytic cycle where substrate is bound adjacent to reduced flavin. Overall, our structural investigation of RebC has revealed two major similarities with the *p*-hydroxybenzoate hydroxylase catalytic cycle: there is a mobile flavin, and the flavin moves IN upon reduction. There are also two key differences from the *p*-hydroxybenzoate hydroxylase catalytic cycle, based on our crystallographic observations: (1) the displacement of the "melting helix" appears to be the conduit for substrate entry and departure, rather than an OPEN conformation of the flavin, likely because of the larger size of RebC's substrate(s), and (2) prior to substrate binding, the FAD in RebC exists in an OUT conformation, in contrast to the OPEN structure for *p*HBH (*26*).

The most intriguing aspect of our reduced flavin structure is the sealing of the "melting helix" without the presence of a bound substrate-like molecule. While the ordering of the helix in the presence of bound hydrophobic molecules can be explained by hydrophobic interactions between the bound molecules and protein residues, such as leucine-358 (Figure 2F), there are no direct contacts between the reduced flavin and helix that can easily explain the ordering of the helix upon change in the redox state of the cofactor and its movement to the IN conformation (Figure 2E). One possible explanation for helix ordering may be that the shift of the flavin conformation drives desolvation, which in turn orders the helix. However, due to the lower number of ordered waters overall in this modest resolution structure, it is difficult to assess this possibility from these structural data. While the molecular explanation for this conformation change remains elusive, the fact that the helix is formed after flavin reduction is certainly suggestive of a key detail in the RebC catalytic cycle: substrate must bind before flavin reduction. Otherwise, flavin reduction will trigger helix formation and substrate will not get in. Substrate binding occurring prior to flavin reduction is also consistent with the *p*-hydroxybenzoate hydroxylase catalytic cycle, where substrate binding causes a 100000-fold increase in the rate of NADPH oxidation (*12*). Although the instability of the proposed RebC substrates has so far prevented us from obtaining the analogous data for RebC, we can compare the rate of FAD reduction without substrate to the rate of overall turnover for the coupled enzyme (StaP/RebC) system in the presence of substrate. The k_{cat} of the coupled enzyme system using chromopyrrolic acid **1** is 0.068 ± 0.01 s^{-1} (*4*). This experiment was carried out using a mixture including StaP (1 μM), RebC (5 μM), NADH (5 mM), spinach ferredoxin (20 μM), flavodoxin NADP$^+$-reductase (1 μM), and FAD (1.7 μM). This turnover rate, which includes reduction and hydroxylation steps, is substantially greater than the rate for FAD reduction of RebC by 1 mM NADH in the absence of substrate (0.0023 s^{-1}) (Supporting Information Table 1). This comparison suggests that substrate binding to RebC must accelerate the rate of flavin reduction by its preferred reductant, NADH, by an order of magnitude. Together with the structural data, this kinetic result suggests that reduction of FAD in the absence of substrate resulting in the ordering of the "melting helix" is unlikely to be physiological relevant and points to a mechanism in which substrate binding to RebC occurs first, ordering the "melting helix" and promoting flavin reduction by NADH.

If the mechanism of RebC includes two hydroxylation steps, one could imagine that the first hydroxylated intermediate that is formed is held in place in the active site by an ordered "melting helix", while the newly reoxidized FAD could swing OUT for rereduction by a second molecule of NADH, in a step that might mimic state 3 of *p*HBH (*8, 13, 28*). Only after the completion of the full reaction would product be released. Regardless of the number of hydroxylation events, the observation that one product is formed when RebC is added to a StaP reaction mixture indicates that accessibility of the active site of RebC must be tightly controlled, and our structural studies suggest that the "melting

helix" is critical to that control. While our structural and kinetic studies show many similarities between RebC and *p*HBH, we do find that RebC adaptations, such as the "melting helix", make it ideally suited to partner with a P450 enzyme, perhaps through a transient interaction during catalysis, accepting and sequestering RebP's reactive product for the exclusive production of the rebeccamycin aglycon.

ACKNOWLEDGMENT

SUPPORTING INFORMATION AVAILABLE

One table and four figures as described in the text. This material is available free of charge via the Internet at http://pubs.acs.org.

REFERENCES

1. Sánchez, C., Butovich, I. A., Braña, A. F., Rohr, J., Méndez, C., and Salas, J. A. (2002) The biosynthetic gene cluster for the antitumor rebeccamycin: characterization and generation of indolocarbazole derivatives. *Chem. Biol. 9*, 519–531.

2. Onaka, H., Taniguchi, S., Igarashi, Y., and Furumai, T. (2003) Characterization of the biosynthetic gene cluster of rebeccamycin from *Lechevalieria aerocolonigenes* ATCC 39243. *Biosci., Biotechnol., Biochem. 67*, 127–138.

3. Sánchez, C., Zhu, L., Braña, A. F., Salas, A. P., Rohr, J., Méndez, C., and Salas, J. A. (2005) Combinatorial biosynthesis of antitumor indolocarbazole compounds. *Proc. Natl. Acad. Sci. U.S.A. 102*, 461–466.

4. Howard-Jones, A. R., and Walsh, C. T. (2006) Staurosporine and rebeccamycin aglycones are assembled by the oxidative action of StaP, StaC, and RebC on chromopyrrolic acid. *J. Am. Chem. Soc. 128*, 12289–12298.

5. Howard-Jones, A. R., and Walsh, C. T. (2007) Nonenzymatic oxidative steps accompanying action of the cytochrome P450 enzymes StaP and RebP in the biosynthesis of staurosporine and rebeccamycin. *J. Am. Chem. Soc. 129*, 11016–11017.

6. Ryan, K. S., Howard-Jones, A. R., Hamill, M. J., Elliott, S. J., Walsh, C. T., and Drennan, C. L. (2007) Crystallographic trapping in the rebeccamycin biosynthetic enzyme RebC. *Proc. Natl. Acad. Sci. U.S.A. 104*, 15311–15316.

7. Ballou, D. P. (2007) Crystallography gets the jump on the enzymologists. *Proc. Natl. Acad. Sci. U.S.A. 104*, 15587–15588.

8. Gatti, D. L., Palfey, B. A., Lah, M. S., Entsch, B., Massey, V., Ballou, D. P., and Ludwig, M. L. (1994) The mobile flavin of 4-OH benzoate hydroxylase. *Science (New York) 266*, 110–114.

9. Enroth, C. (2003) High-resolution structure of phenol hydroxylase and correction of sequence errors. *Acta Crystallogr., Sect. D: Biol. Crystallogr. 59*, 1597–1602.

10. Hiromoto, T., Fujiwara, S., Hosokawa, K., and Yamaguchi, H. (2006) Crystal structure of 3-hydroxybenzoate hydroxylase from *Comamonas testosteroni* has a large tunnel for substrate and oxygen access to the active site. *J. Mol. Biol. 364*, 878–896.

11. Greenhagen, B. T., Shi, K., Robinson, H., Gamage, S., Bera, A. K., Ladner, J. E., and Parsons, J. F. (2008) Crystal structure of the pyocyanin biosynthetic protein PhzS. *Biochemistry 47*, 5281–5289.

12. Ballou, D. P., Entsch, B., and Cole, L. J. (2005) Dynamics involved in catalysis by single-component and two-component flavin-dependent aromatic hydroxylases. *Biochem. Biophys. Res. Commun. 338*, 590–598.

13. Wang, J., Ortiz-Maldonado, M., Entsch, B., Massey, V., Ballou, D., and Gatti, D. L. (2002) Protein and ligand dynamics in 4-hydroxybenzoate hydroxylase. *Proc. Natl. Acad. Sci. U.S.A. 99*, 608–613.

14. Vervoort, J., Van Berkel, W. J., Muller, F., and Moonen, C. T. (1991) NMR studies on *p*-hydroxybenzoate hydroxylase from *Pseudomonas fluorescens* and salicylate hydroxylase from *Pseudomonas putida*. *Eur. J. Biochem./FEBS 200*, 731–738.

15. Moran, G. R., Entsch, B., Palfey, B. A., and Ballou, D. P. (1997) Electrostatic effects on substrate activation in *para*-hydroxybenzoate hydroxylase: studies of the mutant lysine 297 methionine. *Biochemistry 36*, 7548–7556.

16. Otwinowski, Z., and Minor, W. (1997) Processing of X-ray data collected in oscillation mode. *Methods Enzymol. 276*, 307–326.

17. Brünger, A. T., Adams, P. D., Clore, G. M., DeLano, W. L., Gros, P., Grosse-Kunstleve, R. W., Jiang, J. S., Kuszewski, J., Nilges, M., Pannu, N. S., Read, R. J., Rice, L. M., Simonson, T., and Warren, G. L. (1998) Crystallography & NMR system: A new software suite for macromolecular structure determination. *Acta Crystallogr., Sect. D: Biol. Crystallogr. 54*, 905–921.

18. Emsley, P., and Cowtan, K. (2004) Coot: model-building tools for molecular graphics. *Acta Crystallogr., Sect. D: Biol. Crystallogr. 60*, 2126–2132.

19. Dong, C., Flecks, S., Unversucht, S., Haupt, C., van Pee, K. H., and Naismith, J. H. (2005) Tryptophan 7-halogenase (PrnA) structure suggests a mechanism for regioselective chlorination. *Science 309*, 2216–2219.

20. Lyubimov, A. Y., Lario, P. I., Moustafa, I., and Vrielink, A. (2006) Atomic resolution crystallography reveals how changes in pH shape the protein microenvironment. *Nat. Chem. Biol. 2*, 259–264.

21. Kleywegt, G. J., and Jones, T. A. (1997) Model building and refinement practices. *Methods Enzymol. 277*, 208–230.

22. Petøek, M., Otyepka, M., Banáš, P., Košinová, P., Koèa, J., and Damborský, J. (2006) CAVER: a new tool to explore routes from protein clefts, pockets and cavities. *BMC Bioinf. 7*, 316.

23. Patil, P. V., and Ballou, D. P. (2000) The use of protocatechuate dioxygenase for maintaining anaerobic conditions in biochemical experiments. *Anal. Biochem. 286*, 187–192.

24. Katagiri, M., Maeno, H., Yamamoto, S., Hayaishi, O., Kitao, T., and Oae, S. (1965) Salicylate hydroxylase, a monooxygenase requiring flavin adenine dinucleotide. II. The mechanism of salicylate hydroxylation to catechol. *J. Biol. Chem. 240*, 3414–3417.

25. Cole, L. J., Entsch, B., Ortiz-Maldonado, M., and Ballou, D. P. (2005) Properties of *p*-hydroxybenzoate hydroxylase when stabilized in its open conformation. *Biochemistry 44*, 14807–14817.

26. Schreuder, H. A., Prick, P. A., Wierenga, R. K., Vriend, G., Wilson, K. S., Hol, W. G., and Drenth, J. (1989) Crystal structure of the *p*-hydroxybenzoate hydroxylase-substrate complex refined at 1.9 Å resolution. Analysis of the enzyme-substrate and enzyme-product complexes. *J. Mol. Biol. 208*, 679–696.

27. Schreuder, H. A., van der Laan, J. M., Swarte, M. B., Kalk, K. H., Hol, W. G., and Drenth, J. (1992) Crystal structure of the reduced form of *p*-hydroxybenzoate hydroxylase refined at 2.3 Å resolution. *Proteins 14*, 178–190.

28. Schreuder, H. A., Mattevi, A., Obmolova, G., Kalk, K. H., Hol, W. G., van der Bolt, F. J., and van Berkel, W. J. (1994) Crystal structures of wild-type *p*-hydroxybenzoate hydroxylase complexed with 4-aminobenzoate, 2,4-dihydroxybenzoate, and 2-hydroxy-4-aminobenzoate and of the Tyr222Ala mutant complexed with 2-hydroxy-4-aminobenzoate. Evidence for a proton channel and a new binding mode of the flavin ring. *Biochemistry 33*, 10161–10170.

29. Ortiz-Maldonado, M., Cole, L. J., Dumas, S. M., Entsch, B., and Ballou, D. P. (2004) Increased positive electrostatic potential in *p*-hydroxybenzoate hydroxylase accelerates hydroxylation but slows turnover. *Biochemistry 43*, 1569–1579.

30. Brender, J. R., Dertouzos, J., Ballou, D. P., Massey, V., Palfey, B. A., Entsch, B., Steel, D. G., and Gafni, A. (2005) Conformational dynamics of the isoalloxazine in substrate-free *p*-hydroxybenzoate hydroxylase: single-molecule studies. *J. Am. Chem. Soc. 127*, 18171–18178.

31. Moran, G. R., Entsch, B., Palfey, B. A., and Ballou, D. P. (1996) Evidence for flavin movement in the function of *p*-hydroxybenzoate hydroxylase from studies of the mutant Arg220Lys. *Biochemistry 35*, 9278–9285.

32. Entsch, B., Ballou, D. P., and Massey, V. (1976) Flavin-oxygen derivatives involved in hydroxylation by *p*-hydroxybenzoate hydroxylase. *J. Biol. Chem. 251*, 2550–2563.

33. Schreuder, H. A., van der Laan, J. M., Hol, W. G., and Drenth, J. (1988) Crystal structure of *p*-hydroxybenzoate hydroxylase complexed with its reaction product 3,4-dihydroxybenzoate. *J. Mol. Biol. 199*, 637–648.